

Supporting Information

First-Principles Database Driven Computational Neural Network Approach to the Discovery of Active Ternary Nanocatalysts for Oxygen Reduction Reaction

Joonhee Kang, Seung Hyo Noh, Jeemin Hwang, Hoje Chun, Hansung Kim and Byungchan

*Han**

*Department of Chemical and Biomolecular Engineering, Yonsei University, Seoul 03722,
Korea*

Table S1. List of the radial symmetry function (G^2) describing the atomic environments of transition metals in the binary nanoparticles within the cutoff radius $R_c = 6.5 \text{ \AA}$ and $R_{shift} = 0$.

Symmetry functions (G^2)					
No.	Neighboring element	$\eta (\text{\AA}^{-2})$	No.	Neighboring element	$\eta (\text{\AA}^{-2})$
1	Pt	0.001	9	Pt	0.050
2	Ni	0.001	10	Ni	0.050
3	Pt	0.005	11	Pt	0.100
4	Ni	0.005	12	Ni	0.100
5	Pt	0.010	13	Pt	0.200
6	Ni	0.010	14	Ni	0.200
7	Pt	0.020	15	Pt	0.400
8	Ni	0.020	16	Ni	0.400

*Same symmetry functions (G^2) are utilized in PtCu and CuNi systems.

Table S2. List of the angular symmetry function (G^4) describing the atomic environments of transition metals in the binary nanoparticles within the cutoff radius $R_c = 6.5 \text{ \AA}$.

Symmetry functions (G^4)				
No.	Neighbors	$\eta (\text{\AA}^{-2})$	λ	ζ
17-19		0.005	1.0	1.0
20-22		0.005	-1.0	1.0
23-25		0.005	1.0	4.0
26-28		0.005	-1.0	4.0
29-31	Pt-Pt, Ni-Pt, Ni-Ni	0.010	1.0	1.0
32-34		0.010	-1.0	1.0
35-37		0.010	1.0	4.0
38-40		0.010	-1.0	4.0
41-43		0.020	1.0	1.0
44-46		0.020	-1.0	1.0
47-49		0.020	1.0	4.0
50-52		0.020	-1.0	4.0

*Same symmetry functions (G^4) are utilized in PtCu and CuNi systems.

Table S3. List of the radial symmetry function (G^2) describing the atomic environments of transition metals in the ternary nanoparticles within the cutoff radius $R_c = 6.5 \text{ \AA}$ and $R_{shift} = 0$.

Symmetry functions (G^2)					
No.	Neighboring element	$\eta (\text{\AA}^{-2})$	No.	Neighboring element	$\eta (\text{\AA}^{-2})$
1	Pt	0.001	13	Pt	0.050
2	Ni	0.001	14	Ni	0.050
3	Cu	0.001	15	Cu	0.050
4	Pt	0.005	16	Pt	0.100
5	Ni	0.005	17	Ni	0.100
6	Cu	0.005	18	Cu	0.100
7	Pt	0.010	19	Pt	0.200
8	Ni	0.010	20	Ni	0.200
9	Cu	0.010	21	Cu	0.200
10	Pt	0.020	22	Pt	0.400
11	Ni	0.020	23	Ni	0.400
12	Cu	0.020	24	Cu	0.400

Table S4. List of the angular symmetry function (G^4) describing the atomic environments of transition metals in the ternary nanoparticles within the cutoff radius $R_c = 6.5 \text{ \AA}$.

Symmetry functions (G^4)				
No.	Neighbors	$\eta (\text{\AA}^{-2})$	λ	ζ
25-30		0.005	1.0	1.0
31-36		0.005	-1.0	1.0
37-42		0.005	1.0	4.0
43-48	Pt-Pt,	0.005	-1.0	4.0
49-54	Cu-Pt,	0.010	1.0	1.0
55-60	Ni-Pt,	0.010	-1.0	1.0
61-66	Cu-Cu,	0.010	1.0	4.0
67-72	Cu-Ni,	0.010	-1.0	4.0
73-78	Ni-Ni	0.020	1.0	1.0
79-84		0.020	-1.0	1.0
85-90		0.020	1.0	4.0
91-96		0.020	-1.0	4.0

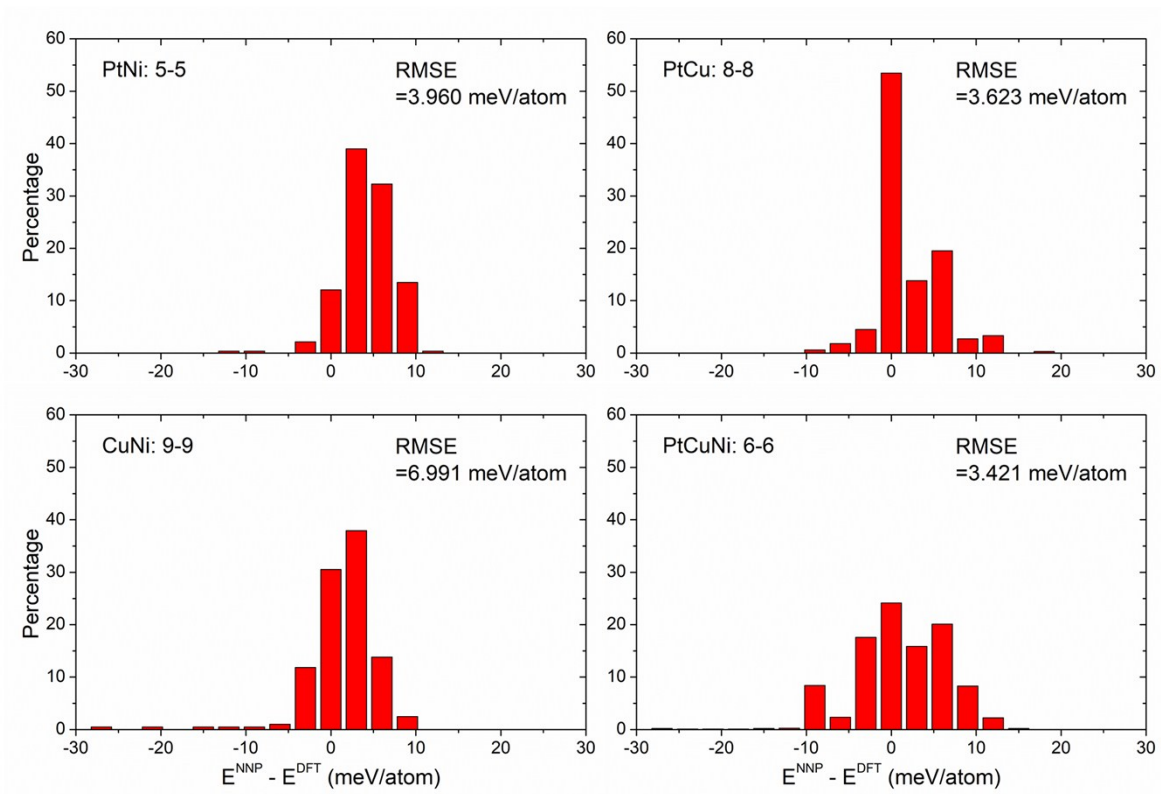


Figure S1. Distribution of the energy difference between NNP and DFT energies for binary and ternary nanoparticles.

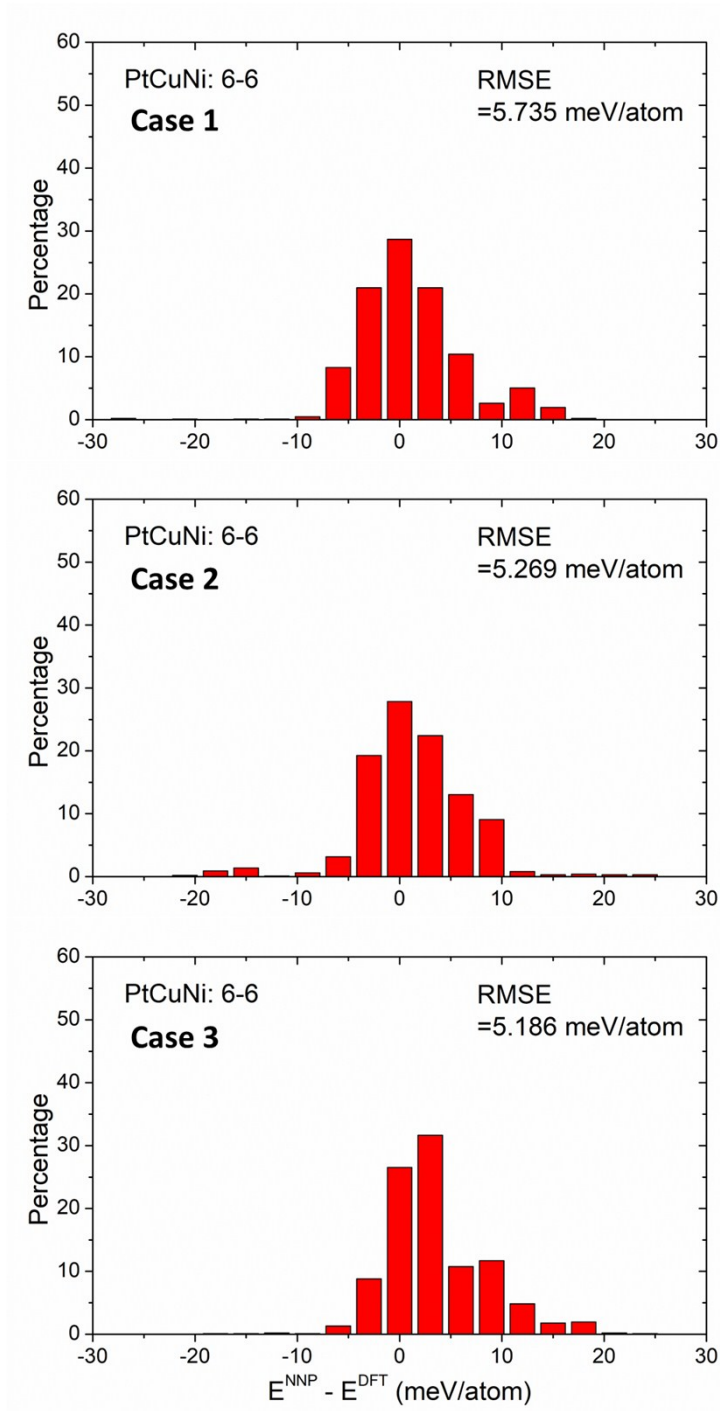
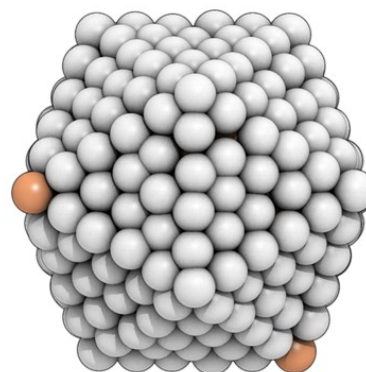
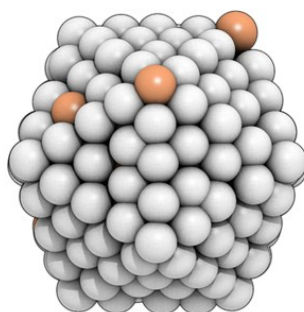
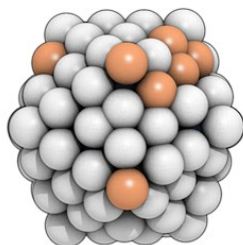


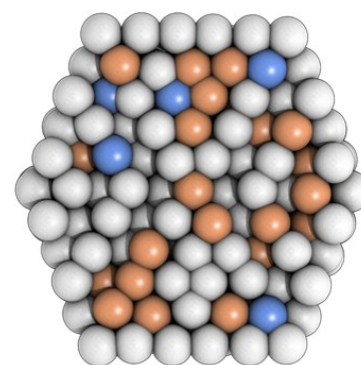
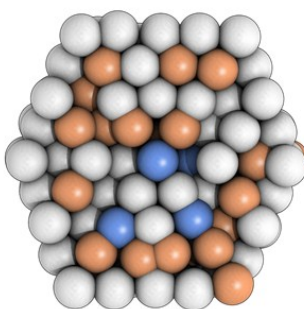
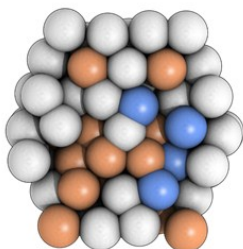
Figure S2. Evaluation of the accuracy of neural network with different training/test set using distribution of the energy difference between NNP and DFT energies for ternary nanoparticles.

Pt7Cu2Ni1

Outside View



Inside View



Pt₁₀₂Cu₃₀Ni₁₅

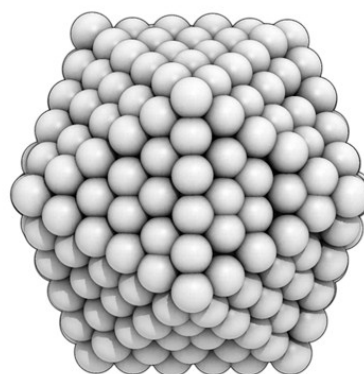
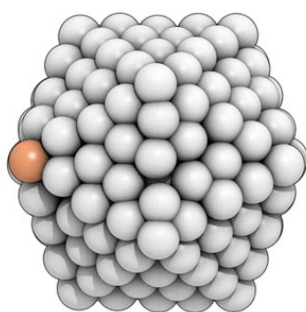
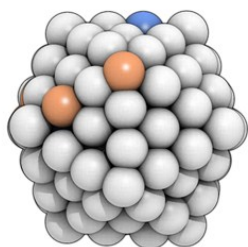
Pt₂₁₆Cu₆₂Ni₃₁

Pt₃₉₃Cu₁₁₂Ni₅₆

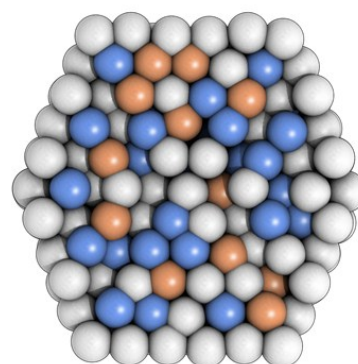
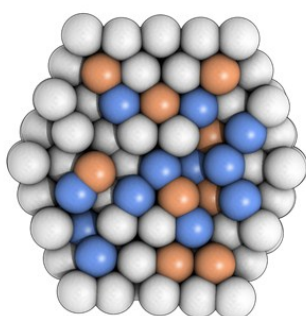
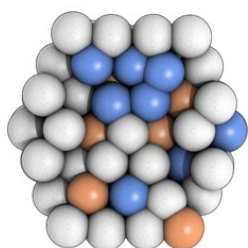
Figure S3. The outside and inside atomic arrangements of Pt7Cu1Ni1 nanoparticles from MC/MD simulations.

Pt7Cu1Ni2

Outside View



Inside View



Pt₁₀₂Cu₁₅Ni₃₀

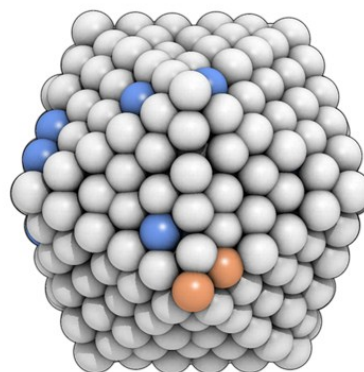
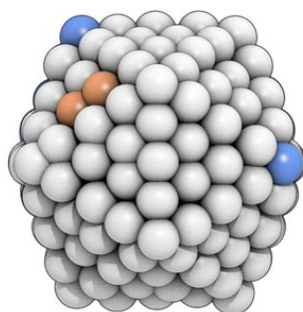
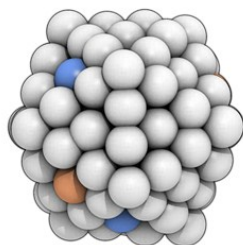
Pt₂₁₆Cu₃₁Ni₆₂

Pt₃₉₃Cu₅₆Ni₁₁₂

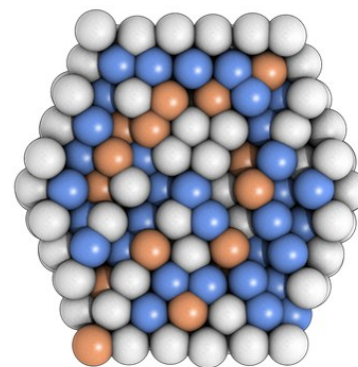
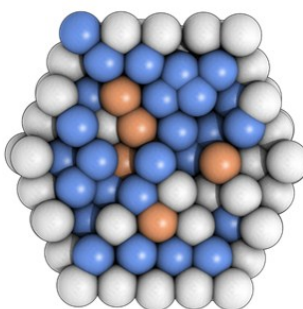
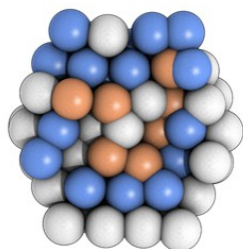
Figure S4. The outside and inside atomic arrangements of Pt7Cu1Ni2 nanoparticles from MC/MD simulations.

Pt6Cu1Ni3

Outside View



Inside View



Pt₈₇Cu₁₅Ni₄₅

Pt₁₈₅Cu₃₁Ni₉₃

Pt₃₃₇Cu₅₆Ni₁₆₈

Figure S5. The outside and inside atomic arrangements of Pt6Cu1Ni3 nanoparticles from MC/MD simulations.

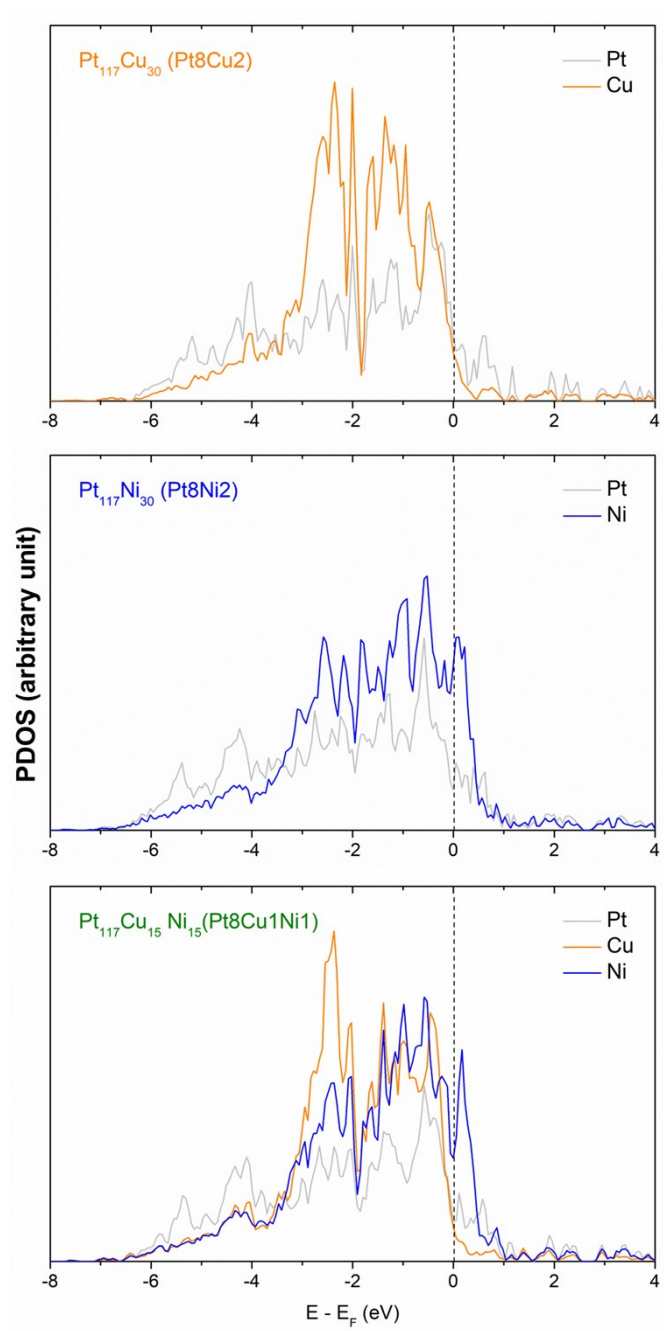


Figure S6. PDOS (*d* orbital) of Pt in the outermost shell and Cu or Ni in the core of $M_{55}@Pt_{92}$ nanoparticles with respect to the Fermi level, E_F .

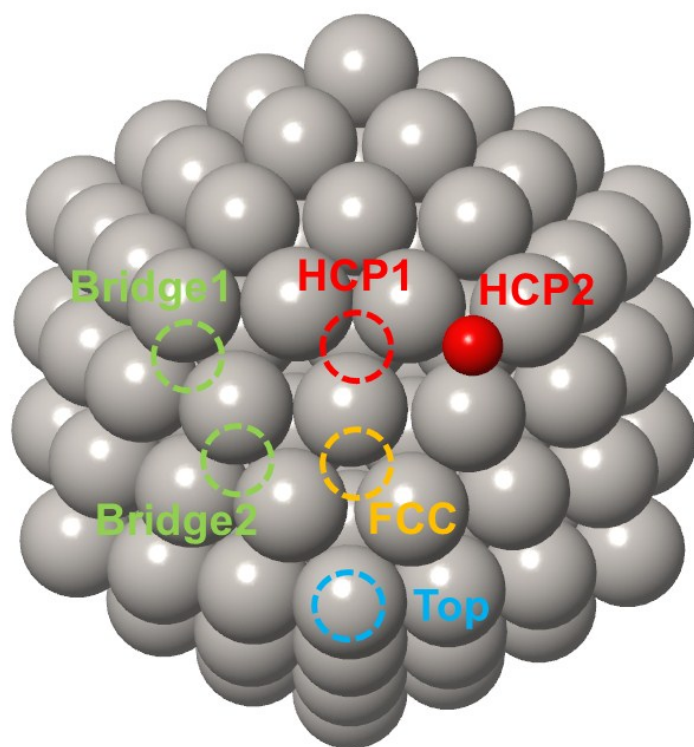


Figure S7. Oxygen adsorption sites on the outermost shell of nanoparticles. HCP2 is thermodynamically favorable oxygen adsorption site.